



## Structural behaviour of masonry arch with no-horizontal springing settlement

P. Zampieri, N. Simoncello, C. Pellegrino

Department of Civil, Environmental and Architectural Engineering, University of Padova, Via Marzolo, 9 - 35131 Padova, Italy  
paolo.zampieri@dicea.unipd.it, <http://orcid.org/0000-0002-4556-5043>

**ABSTRACT.** This paper presents a calculation procedure for assessing the structural integrity of a masonry arch with non-horizontal springing settlement. By applying the Principle of Virtual Work (PVW) to the deformed arch system, the procedure proposed herein details the reaction forces and thrust lines for each step of imposed settlement of the support. The procedure can also be used estimate the final displacement that causes complete failure of arch structural capacity.

The results of the analysis procedure were compared against those obtained by experimental testing so as to validate the proposed calculation method.

**KEYWORDS.** Safety of masonry arches; Collapse mechanism; Springing settlement; Experiment.



**Citation:** Zampieri, P., Simoncello, N., Pellegrino, C., Structural behavior of masonry arch with no-horizontal springing settlement, *Frattura ed Integrità Strutturale*, 43 (2018) 182-190.

**Received:** 18.11.2017

**Accepted:** 28.11.2017

**Published:** 01.01.2018

**Copyright:** © 2018 This is an open access article under the terms of the CC-BY 4.0, which permits unrestricted use, distribution, and reproduction in any medium, provided the original author and source are credited.

### INTRODUCTION

Assessment of the structural integrity of masonry arch structures is highly important, as the arch represents the main structural element of many existing constructions (bridges and buildings) both in Europe and around the world. Consequently, the structural behaviour of masonry arches continues to be subject of scientific research. The first modern studies on the structural behaviour of masonry arch structures were conducted by Heyman [1], who introduced simplified hypotheses for the application of equilibrium limit analysis to assess the load-carrying capacity of such structures. Heyman's work gave rise to numerous subsequent studies that assessed the main aspects affecting the structural response of masonry arches. In particular, recent studies have focused attention on the dynamic [2-6] and seismic behaviour [7-20] of existing masonry arch structures.

One structural problem that has been rather neglected [21-24] in recent studies involves the behaviour of arches as a result of imposed settlement to the supports. The behaviour of arches with horizontal settlement has been comprehensively studied both by applying limit analysis [22-24] and through experimental testing [22]. Nonetheless, the structural behaviour of masonry arches undergone a non-horizontal displacement of supports is still partially unexplored. The study of masonry arch resistance to the imposed settlement of supports is important, as this type of stress can be found in existing structures. For example, in masonry arch bridges, settlement of the arch supports may occur due to loss of load carrying capacity of the subsoil. Another example is steel ties in historical buildings, used to counteract the horizontal thrust of arch. If damaged, these can be cause of settlement of arch springing.



Referring to the main studies about horizontal displacement available in literature, Ochsendorf [22] analyzed the formation of cracks of a masonry arch in relation to the horizontal thrust and the distinctive geometrical characteristics of the structure, that are thickness  $t$ , radius  $R$  and angle of embrace  $\beta$ , through thrust line analysis. Coccia et al. [23] reviewed the Ochsendorf's work suggesting an innovative method in studying these phenomena based on the implementation of kinematic theorem to deformed configuration of the arch. In particular, they showed that the considered collapse configuration for the masonry arch, then the position of the cracks, depend on the displacement imposed to the supports. Hence all the studies conducted focused on the collapse mechanism for the horizontal displacement, the aim of this paper is to analyze others settlements condition. In particular, an imposed displacement with two different direction components that are horizontal and vertical. For these reasons, the purpose of this work is to amplify the already available investigations in settlement springing of masonry archs analyzing other settlement condition, to develop the arch behavior knowledge. Throughout limit analysis and experimental testing, the structural behaviour of masonry arches subjected to a  $d_k$  settlement of springing on an inclined direction  $\alpha$  of  $45^\circ$  (Fig. 1) is investigated.

Moreover, knowing that the cracks position in a collapse configuration may vary increasing the settlement, as already stated throughout FEM and experimental analysis, this behaviour has been analyzed for a  $45^\circ$  direction settlement direction by means of a Limit Analysis then compared with the field test.

The analysis procedure used to assess the thrust line and reaction forces of the springing will be described in detail for each incremental displacement value  $d_k$ , until reaching the condition of complete collapse of the arch. This procedure uses: i) limit analysis in the hypotheses of significant arch displacements, and ii) analysis of thrust lines.

Following this, the results of experimental testing on a masonry arch with mortar joints subjected to one of two springings incremental settlement (inclination equal to  $45^\circ$ ) will be presented. As will be illustrated, the comparison of analytical results and experimental results demonstrates the great predictive ability of the calculation model developed.

#### ANALYSIS OF MASONRY ARCHES WITH NON-HORIZONTAL SPRINGING SETTLEMENT

When a masonry arch loses a degree of freedom (and may be displaced along a given direction  $\alpha$ ), a collapse mechanism is created, with three cracking hinges (Fig. 1) and the thrust line within the form of the arch is tangential to the edge at the three hinge points. This three-hinge mechanism is created as a result of small movements along the  $\alpha$  direction. Thus, assuming that the displacement in the  $\alpha$  direction that triggers the collapse mechanism is null, it is possible to: remove the constraint condition in direction  $\alpha$  and replace it with an equivalent reaction force  $R_{\alpha,0}$  (Fig.1); define a three-hinge collapse mechanism and an associated field of virtual displacements (Fig. 1) and apply PVW using Heyman's hypotheses [1].

For an arch consisting of  $n$  blocks, assuming any initial position of hinges 1, 2, 3 (Fig. 1), it is possible to define the external work of gravitational forces  $g_i$  and the force  $R_{\alpha,0}$  as:

$$L_e = \sum_{i=1}^n g_i \cdot \delta v_i + R_{\alpha,0} \cdot \delta_s(x_0, y_0) = 0 \tag{1}$$

where:

$g_i$  is the gravitational force applied to each  $i$ -rigid block of the arch;

$v_i$  is the vertical virtual displacement due to  $g_i$  applied to each  $i$ -rigid block of the arch.

$s(x_0, y_0)$  is the virtual displacement of the settled springing.

From (1), the value of the support reaction force  $R_{\alpha,0}$  can be obtained, as follows:

$$R_{\alpha,0} = \frac{\sum_{i=1}^n g_i \cdot \delta v_i}{\delta_s(x_0, y_0)} \tag{2}$$

Once the value of  $R_{\alpha,0}$  is known, it is possible to: define the thrust line following the procedure shown in Zampieri et al 2016 [10], determine a new updated position of the three cracking hinges and apply PVW again. Repeating this process, convergence is reached when the solution sought is both statically and kinematically admissible at the same time. This

condition defines the positions  $(X_{1,0}; Y_{1,0})$   $(X_{2,0}; Y_{2,0})$   $(X_{3,0}; Y_{3,0})$  of the three hinges of the collapse mechanism in the initial configuration  $\Omega_0$  corresponding (ideally) to zero settlement of the movable springing and the minimum reaction force  $R_{\alpha,0}$ . Subsequently, it is possible to apply a generic displacement  $d_k$  of the movable springing along a generic direction at the initial condition  $\Omega_0$  and then reapply PVW to the new deformed configuration  $\Omega_k$  (the subscript  $k$  refers to the  $k$ -th increment of displacement  $d_k$ ) in order to determine the updated value  $R_{\alpha,k}$  of the reaction force in the  $\alpha$  direction. Then a new thrust line is defined, verifying whether the solution sought is statically and kinematically admissible (that is, the thrust line is contained within the form of the arch and is tangential to the edge at the hinge points).

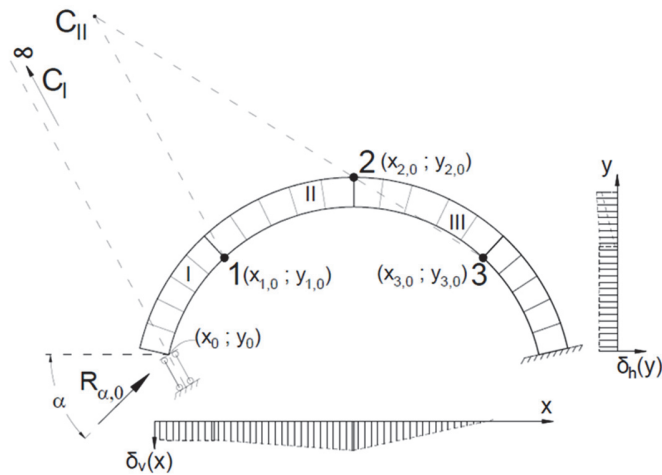


Figure 1: Virtual displacement diagrams in the initial configuration of the masonry arch.

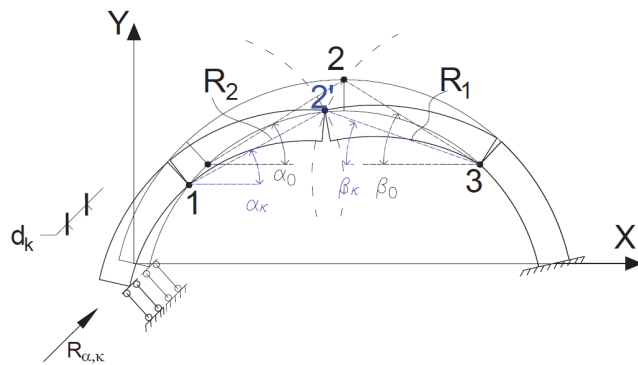


Figure 2: Representation of the kinematic mechanism in the generic configuration displaced by  $\Omega_k$ .

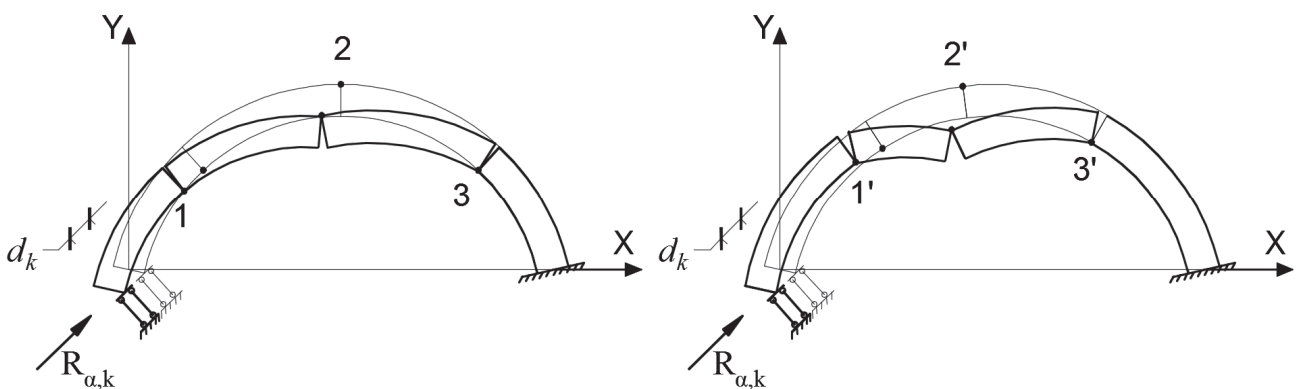


Figure 3: Condition in which the hinges calculated in the  $k-1$ -th iteration do not coincide with the hinges in the  $k$ -th iteration



If this condition is not verified, the hinge points (1, 2 and 3) are moved to the local maximum and minimum points of the thrust line before applying PVW again. This procedure is reiterated until the thrust line condition is verified. It should be emphasised that for a given displacement  $d_k$  the hinges may not be correctly positioned (1, 2, 3) in relation to the displacement in the previous step  $d_{k-1}$ , but rather the hinge positions are updated (1', 2', 3') as shown in Fig. 3. This procedure can therefore assess (step-by-step) whether the collapse hinge positions have changed (Fig. 3) as the displacement  $d_k$  increases.

The procedure described is repeated for incremental values of  $d_k$  and ends when the arch collapse condition is verified due to alignment of the three crack hinges. Fig. 4 shows a flow chart of the algorithm described above.

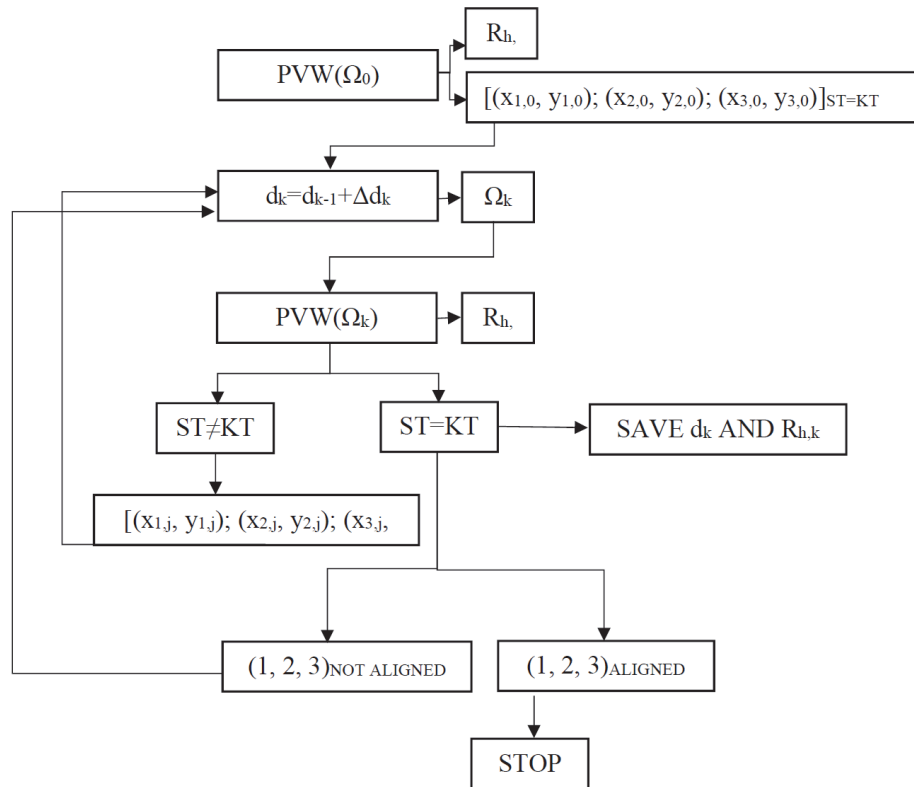


Figure 4: Algorithm implemented.

## EXPERIMENTAL TESTING

Experimental analysis was carried out on a masonry arch made of solid bricks bound with traditional mortar. A plastic caisson was used in order to obtain a great geometrically regular element instead of using bricks without mortar as in Ochsendorf [22] tests. The mortar employed for this experimental has low tensile property according with the hypothesis assumed by Clemente [26]. The masonry arch was fixed to a steel frame with a movable springing along a  $45^\circ$  direction (Fig. 5). This applied displacement system represents an innovative case never studied before by other authors. The arch made from 37 bricks measuring  $250 \times 125 \times 50 \text{ mm}^3$  has a span length of 2281 mm, an arch rise of 585 mm and an embrace angle ( $\beta$ ) equal to  $107.356^\circ$ . Fig. 5 shows the experimental test diagram and the graphical representation of the mechanical system capable of applying an incremental displacement along an inclined direction of  $45^\circ$ , providing instant-by-instant the imposed displacement value.

### Results of experimental testing

During the test, images were continuously recorded that allowed the displacement imposed by the mechanical system to be associated with the configuration of the arch collapse mechanism (Fig. 6). Specifically, in the images shown in Fig. 6, three different collapse mechanism configurations can be identified for different values of displacement  $d_k$ , as shown in the graph in Fig. 9.

All three initial cracking hinges were created at a displacement equal to 2.7 mm at joint 3, joint 18 and joint 34. During the test, it was seen that up until a certain displacement of  $d_k = 153.6$  mm, the configuration of the hinges remained unchanged (Fig. 7a) in relation to the initial configuration. At a displacement of 153.6 mm (Fig. 7b), hinge 3 shifted from position 34 to position 33, and hinges 1 and 2 remained unchanged. As the displacement increased, at 165.1 mm (Fig. 7c), hinge 1 instantly shifted from position 3 to position 7, hinge 3 instantly shifted from position 33 to position 30, and hinge 1 remained unchanged. Following this, the configuration of the hinges remained unchanged until alignment of the three hinges at the instant in which the arch collapsed (Fig. 7d).

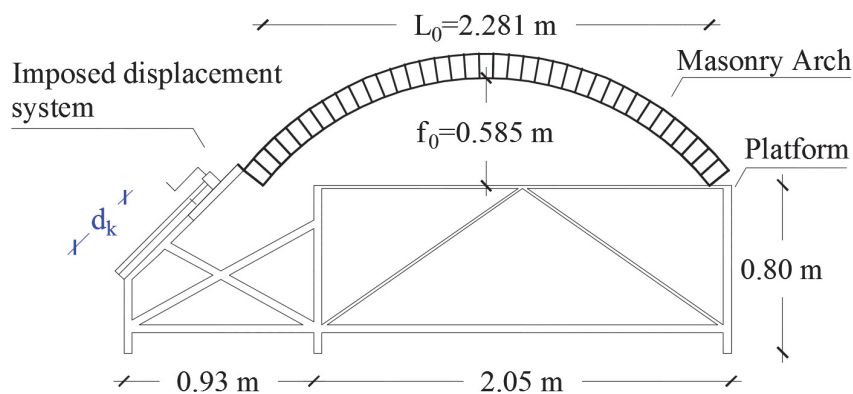


Figure 5: Configuration of the specimen.

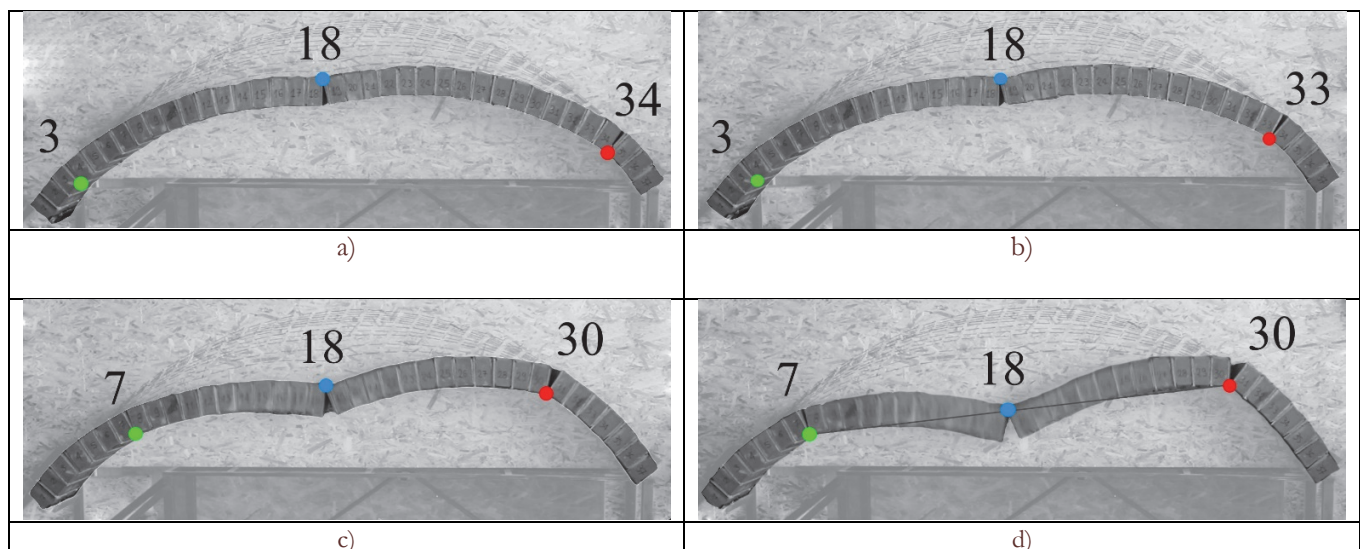


Figure 6: Collapse mechanism configuration of experimental arch specimen

## COMPARISON BETWEEN LIMIT ANALYSIS AND EXPERIMENTAL TESTING

Using the proposed calculation procedure, it was possible to analytically simulate the behaviour of the experimental test. This section provides a comparison of the experimental results with the analytical results. In particular, the images shown in Fig. 7 illustrate the four cracking hinge configurations extracted from the calculation program, highlighting that the shifts in the position of the cracking hinges as displacement  $d_k$  increases, found during the experimental test, are also identified in limit analysis. This result is confirmed by analysis of the graph in Fig. 9a, which compares the variation in the position of the cracking hinges ( $n_i$ ;  $i = 1,2,3$ ) according to the displacement  $d_k$  through comparison of the four curves relating to experimental testing and four curves relating to limit analysis. Specifically, limit analysis allows four different cracking hinge configurations to be identified:



Configuration 1:  $n_1=1$   $n_2=18$   $n_3=36$ ;  $0 \leq d_k \leq 176$   
 Configuration 2:  $n_1=4$   $n_2=18$   $n_3=35$ ;  $176 \leq d_k \leq 189.2$   
 Configuration 3:  $n_1=4$   $n_2=18$   $n_3=31$ ;  $189.2 \leq d_k \leq 193.6$   
 Configuration 4:  $n_1=6$   $n_2=18$   $n_3=31$ ;  $193.6 \leq d_k \leq 220$

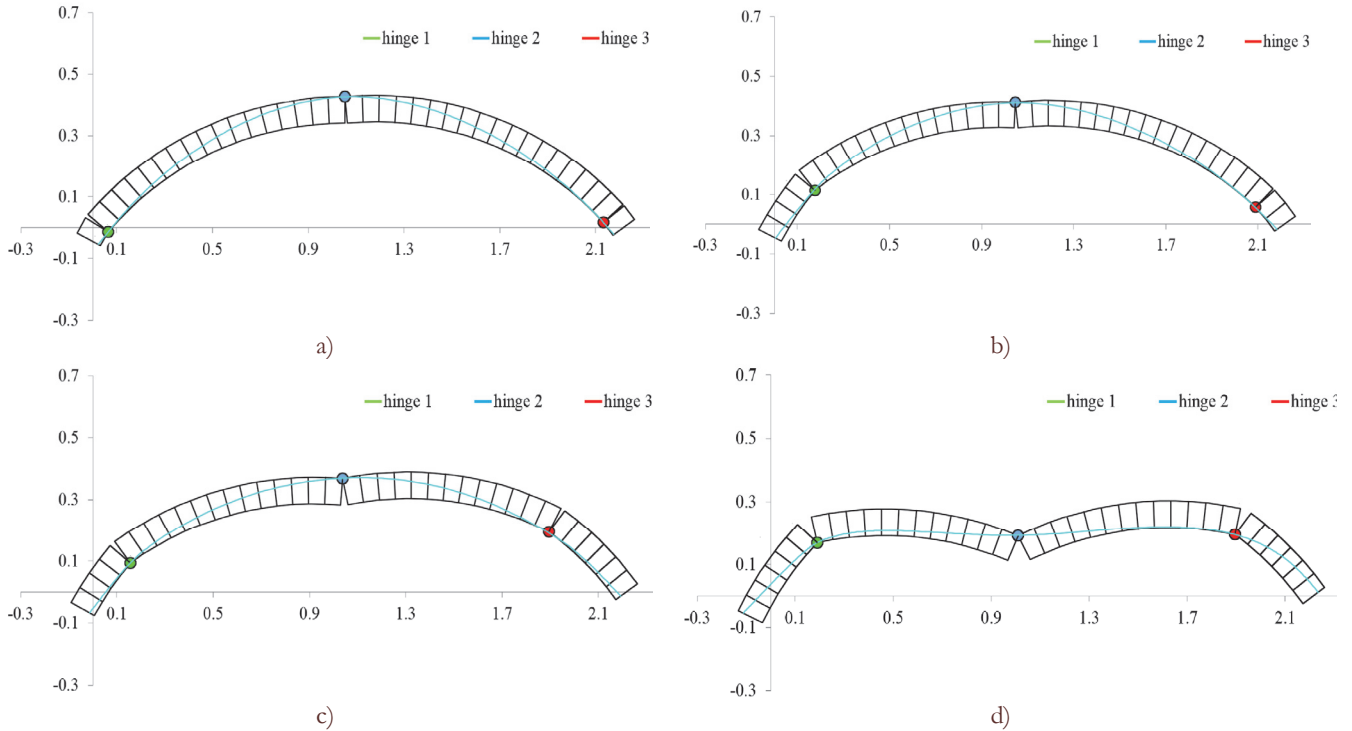


Figure 7: Collapse mechanism configurations of limit analysis arch model

As can be deduced from the graph shown in Fig. 8, which compares the different hinge configurations obtained from experimental testing against those obtained from limit analysis, the result of experimental testing and limit analysis do not coincide perfectly. The discrepancies however can be considered acceptable and are attributable to intrinsic uncertainties in the parameters that define the structural response of real structures:

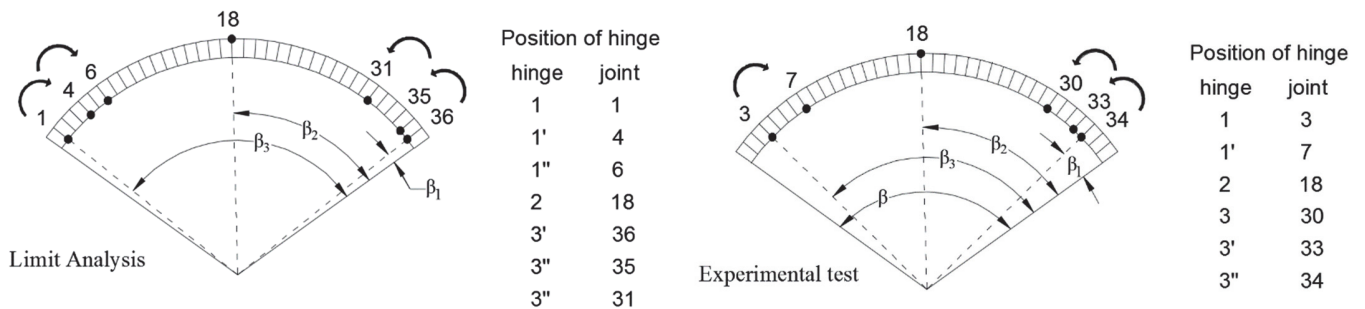


Figure 8: Comparison of Configurations of cracking hinges carried out from. a) Limit Analysis and b) Experimental testing

- uncertainties and/or irregularities in defining the geometry of the specimen [20]
- irregularities due to masonry and mortar production processes
- errors and uncertainties relating to how the test is conducted.

It is interesting to observe from the graph in Fig. 9a that up to a displacement  $d_k$  equal to approximately eighty percent of the final displacement, the hinges remain unchanged in the final configuration. Their positions in fact change in a range of displacements  $d_k$  between eighty and ninety percent of the collapse displacement.

Fig. 9b shows the curve that correlates the displacement  $d_k$  with the reaction force  $R_{\alpha,k}$ , which increases continually and exponentially up to the maximum displacement, at which point the tangent of the curve is vertical. It is also important to note that the final displacement obtained from limit analysis is 14.7% higher than the displacement seen in experimental testing (dotted line in Fig. 9b). If the intrinsic geometric irregularities of real arches were able to be taken into account in the calculation procedure developed, the final displacement (in limit analysis) would most likely be closer to the value obtained in experimental testing.

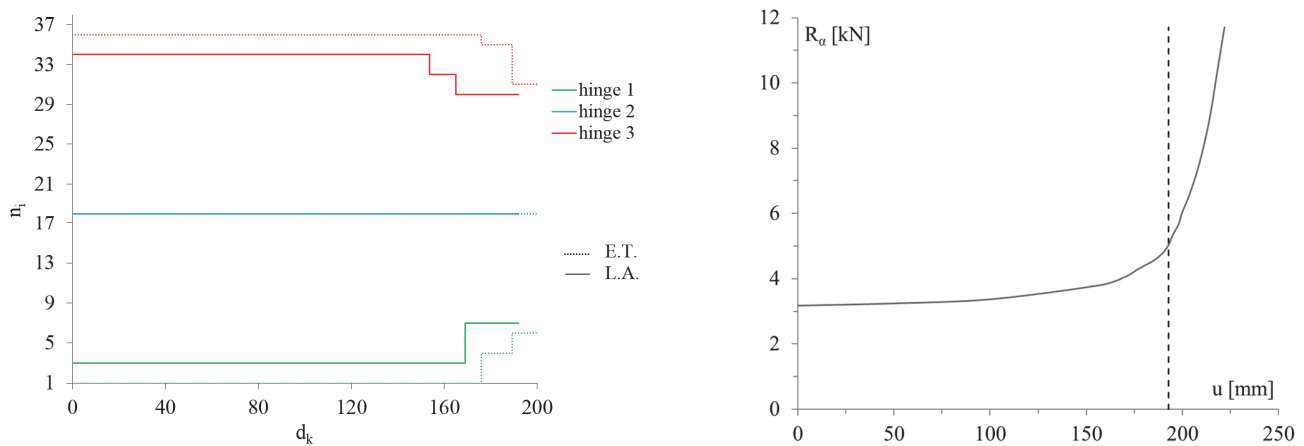


Figure 9: a) Position of hinges as a function of  $d_k$  b) Capacity curve.

## CONCLUSIONS

This paper examines the behaviour of a masonry arch subjected to settlement along a direction  $\alpha$ . The innovation of this paper lies in analyzing collapse mechanisms for the horizontal settlement condition, despite what other studies have already considered. Other previous studies about horizontal settlement only led to a mechanism classification introducing a FEM simulation analysis. This paper investigates on a different configuration, comparing the simulation in terms of limit analysis and implementing the possibility of a varying collapse mechanism configuration.

Using the method of equilibrium limit analysis with the hypothesis of significant displacements, an algorithm is proposed that uses PVW. The purpose was to analyse the thrust line and to identify the different positions of collapse hinges occurred on the arch, from the initial configuration corresponding to null displacement of the stringing, up to the final collapse configuration. A real arch was built to conduct an experimental test by subjecting it to springing settlement along an inclined direction of  $45^\circ$  until collapse. As the value of imposed displacement was increased, the various configurations of the deformed arch were continuously recorded.

The results of the experimental test confirmed the reliability of the structural model developed. However, there were discrepancies in the position of the cracking hinges under displacement. Such discrepancies can be attributed to the geometrical irregularities of the arch and the inherent uncertainties in real structures.

In conclusion, as Fig.8 shows, the limit analysis induces the development of an additional crack at joint 6 in the fourth collapse configuration contrary to what the experimental evidence shows, where the position of hinges is preserved for the same configuration. As Fig. 9 shows, in the limit analysis the last displacement of the springing results greater compared to experimental response. This is considered to be due to the fact that the cracks  $n_1$  and  $n_2$  are located between a different and greater number of voussoirs compared to real case. Therefore, the alignment of the three hinges is verified in conjunction with a greater last displacement. As already stated, this discrepancy can be reduced introducing an inherent uncertainties factor.



## REFERENCES

- [1] Heyman, J., The safety of masonry arches, *Int J. Mech Sci.*, 11 (1969) 363-385.
- [2] De Lorenzis, L., DeJong, M., Ochsendorf, J., Failure of masonry arches under impulse base motion, *Earthq Eng Struct Dyn.*, 36 (2007) 2119–2136.
- [3] Misseri, G., Rovero, L., Parametric investigation on the dynamic behaviour of masonry pointed arches, *Archive of Applied Mechanics.*, 87 (3) (2017) 385-404.
- [4] Ramaglia, G., Lignola, G.P., Prota, A., Collapse analysis of slender masonry barrel vaults, *Engineering Structures.*, 117 (2016) 86-100.
- [5] Gaetani, A., Lourenço, P.B., Monti, G., Moroni, M., Shaking table tests and numerical analyses on a scaled dry-joint arch undergoing windowed sine pulses, *Bulletin of Earthquake Engineering.*, 15 (11) (2017) 4939-4961.
- [6] Zampieri, P., Zanini, M.A., Zurlo, R., Seismic behaviour analysis of classes of masonry arch bridges, *Key Engineering Materials.*, 628 (2014) 136-142. DOI: 10.4028/www.scientific.net/KEM.628.136.
- [7] da Porto, F., Tecchio, G., Zampieri, P., Modena, C., Prota, A., Simplified seismic assessment of railway masonry arch bridges by limit analysis, *Structure and Infrastructure Engineering.*, 12 (5) (2016) 567-591. DOI: 10.1080/15732479.2015.1031141.
- [8] De Santis, S., de Felice, G., A fibre beam based approach for the evaluation of the seismic capacity of masonry arches, *Earthquake Engineering and Structural Dynamics.*, 43 (2014) 1661-1681.
- [9] Dimitri, R., Tornabene, F., A parametric investigation of the seismic capacity for masonry arches and portals of different shapes, *Engineering Failure Analysis*, 52 (2015) 1-34.
- [10] Zampieri, P., Zanini, M.A., Faleschini, F., Influence of damage on the seismic failure analysis of masonry arches, *Construction and Building Materials.*, 119 (2016) 343-355. DOI: 10.1016/j.conbuildmat.2016.05.024
- [11] Zampieri, P., Zanini, M.A., Faleschini, F., Derivation of analytical seismic fragility functions for common masonry bridge types: methodology and application to real cases, *Engineering Failure Analysis.*, 68 (2016) 275-291. DOI: 10.1016/j.engfailanal.2016.05.031
- [12] M. S. Marefat, M. Yazdani, and M. Jafari., Seismic assessment of small to medium spans plain concrete arch bridges, *European Journal Of Environmental And Civil Engineering.*, (2017). DOI: 10.1080/19648189.2017.1320589.
- [13] Zampieri, P., Zanini, M. A., Modena, C., Simplified seismic assessment of multi-span masonry arch bridges, *Bulletin of Earthquake Engineering.*, (2015). DOI 10.1007/s10518-015-9733-2.
- [14] Zampieri, P., Tecchio, G., da Porto, F., Modena, C., (2015). Limit analysis of transverse seismic capacity of multi-span masonry arch bridges, *Bulletin of Earthquake Engineering.*, 13(5) (2015) 1557-152. DOI 10.1007/s10518-014-9664-3.
- [15] Cavalagli, N., Gusella, V., Severini, L., Lateral loads carrying capacity and minimum thickness of circular and pointed masonry arches, *Int J Mech Sci.*, 115–116 (2016) 645–56.
- [16] Sayin, E., Nonlinear seismic response of a masonry arch bridge, *Earthquake and Structures.*, 10 (2) (2016) 483-494. DOI: 10.12989/eas.2016.10.2.483.
- [17] Michiels, T., Adriaenssens, S., Form-finding algorithm for masonry arches subjected to in-plane earthquake loading, *Computers and Structures.*, 195 (2018) 85-98. DOI: 10.1016/j.compstruc.2017.10.001.
- [18] Tecchio, G., Da Porto, F., Zampieri, P., Modena, C., Bettio, C., Static and seismic retrofit of masonry arch bridges: Case studies, *Bridge Maintenance, Safety, Management, Resilience and Sustainability - Proceedings of the Sixth International Conference on Bridge Maintenance, Safety and Management.*, (2012) 1094-1098.
- [19] Conde, B., Ramos, L.F., Oliveira, D.V., Riveiro, B., Solla, M., Structural assessment of masonry arch bridges by combination of non-destructive testing techniques and three-dimensional numerical modelling: Application to Vilanova bridge, *Engineering Structures*, 148 (2017) 621-638. DOI: 10.1016/j.engstruct.2017.07.011.
- [20] Cavalagli, N., Gusella, V., Severini, L., The safety of masonry arches with uncertain geometry, *Computers and Structures.*, 188 (2017) 17-31. DOI: 10.1016/j.compstruc.2017.04.003
- [21] Zampieri, P., Zanini, M.A., Faleschini, F., Hofer, L., Pellegrino, C., Failure analysis of masonry arch bridges subject to local pier scour, *Engineering Failure Analysis*, 79 (2017) 371-384. DOI: 10.1016/j.engfailanal.2017.05.028.
- [22] Ochsendorf, J.A., The masonry arch on spreading supports, *Struct Eng Inst Struct Eng Lond.*, 84(2) (2006) 29–36.
- [23] Coccia, S., Di Carlo, F., Rinaldi, Z., Collapse displacements for a mechanism of spreading-induced supports in a masonry arch, *International Journal of Advanced Structural Engineering.*, 7(3) (2015) 307-320. DOI: 10.1007/s40091-015-0101-x.
- [24] Como, M., On the role played by Settlements in the statics of masonry structures, In: *The conference on geotechnical engineering for the preservation of monuments and historic sites, Napoli, Italy, October, Balkema, Rotterdam, (1996) 3–4.*





- [25] Severini, L., Cavalagli, N., Zampieri, P., Simoncello, N., Gusella, V., Pellegrino C., Effects of spread and local geometrical irregularities on the horizontal carrying capacity of masonry arches, *Atti del XVII Convegno ANIDIS L'ingegneria Sismica in Italia*, (2017) 27-33.
- [26] Clemente, P., Saitta, F. Analysis of No-Tension Material Arch Bridges with Finite Compression Strength *Journal of Structural Engineering*, 143(1) (2017).

## NOMENCLATURE

$d_k$	Displacement of the settlement of the support on the current step;
$d_{k-1}$	Displacement of the settlement of the support on the previously step;
$\Delta d_k$	Different of the displacement between two next steps;
$R_{\alpha,0}$	Reaction force in the $\alpha$ direction at the undamaged condition of the arch;
$R_{\alpha,k}$	Reaction force in the $\alpha$ direction at the damage condition of the arch on the current step;
$\alpha$	Direction angle of the settlement
PVW	Principle of the Virtual Work
$g_i$	Gravitational force applied to each i-rigid block of the arch;
$v_i$	Vertical virtual displacement due to $g_i$ applied to each i-rigid block of the arch;
$s(X_0, Y_0)$	Virtual displacement of the settled springing;
$\Omega_0$	Initial configuration of the arch;
$\Omega_k$	Configuration of the arch on the current step;
ST	Static condition of the arch;
KT	Kinematic condition of the arch.